JOURNAL OF SOLID STATE CHEMISTRY **141,** 554–561 (1998)
ARTICLE NO. SC988018

Magnetic Properties of Metastable Lithium Iron Oxides Obtained by Solvothermal/Hydrothermal Reaction

Mitsuharu Tabuchi,[1] Kazuaki Ado, Hironori Kobayashi, Ichiro Matsubara, and Hiroyuki Kageyama

Osaka National Research Institute, 1-8-31, Midorigaoka, Ikeda, Osaka 563, Japan

Masayuki Wakita, Satoshi Tsutsui, and Saburo Nasu

Faculty of Engineering Science, Osaka University, 1-3, Machikaneyama, Toyonaka, Osaka 560, Japan

Yasuo Takeda

Faculty of Engineering, Mie University, Tsu, Mie 514, Japan

Christian Masquelier

Universite Paris-XI Orsay, Batiment 414, 91405 Orsay Cedex, France

and

Atsushi Hirano and Ryoji Kanno

Faculty of Science, Kobe University, Rokkoudai, Nada, Kobe, Hyogo 657, Japan

Received March 12, 1998; in revised form July 14, 1998; accepted July 24, 1998

The magnetic properties of metastable lithium iron oxides obtained by solvothermal ion-exchange and mixed-alkaline hydrothermal reactions have been examined. Fe^{2+}-containing $Li_{1-x}Fe_{5+x}O_8$ with inverse spinel structure have been obtained from a mixture of LiCl and α-$NaFeO_2$ by solvothermal reaction. The phase has spontaneous magnetization at 300 K and decompose readily by heating at 400°C in air. Metastable layered $LiFeO_2$ with a small amount of α-$LiFeO_2$ could be obtained from α-FeOOH and KOH–LiOH mixed-alkaline solution by hydrothermal reaction. The layered polymorph exhibited antiferromagnetic behavior ($T_N = 20$ K) but no spin-glass-like behavior, as observed previously for $LiNiO_2$. © 1998 Academic Press

1. INTRODUCTION

$LiFe_5O_8$ with inverse spinel structure and $LiFeO_2$ with rock salt related structure have been regarded as equilibrium phases for lithium ferrites. The spinel ferrite is a magnetic material due to its ferrimagnetism. $LiFeO_2$ has become attractive as a cathode material for rechargeable lithium batteries because lithium iron oxides are inexpensive and less toxic compared to Co and Ni in $LiCoO_2$ and $LiNiO_2$. However, neither Li extraction nor Li insertion has been reported for the cubic and cation-disordered α (1), tetragonal cation-disordered β (1), monoclinic cation-ordered β (2), and tetragonal cation-ordered γ polymorphs (3) which could be obtained by ordinary solid-state reaction. Several authors tried to prepare metastable $LiFeO_2$ by selecting mild preparation conditions (soft-chemical reaction) below 500°C. $LiFeO_2$ polymorphs with corrugated layer (4) and goethite type (5) structures could be isolated from γ- and α-FeOOH, respectively, by ion-exchange reaction and can act as cathode materials. Other researchers have reported the preparation of metastable layered $LiFeO_2$ isostructural with $LiCoO_2$ and $LiNiO_2$ (α-$NaFeO_2$ type structure) by topotactic ion-exchange reaction of α-$NaFeO_2$ with Li^+-containing molten salts (6–9). LiO_6 and FeO_6 slabs are alternately stacked perpendicular to the [001] direction of the hexagonal unit cell in layered $LiFeO_2$. However, the ion-exchanged samples contain a minor amount of spinel phase, indicating that ideal ion-exchange reaction was not accomplished (9). Recently, we succeeded in obtaining this polymorph directly from Fe^{3+} sources (either α-FeOOH or $FeCl_3$-$6H_2O$) using a mixed-alkaline (either LiOH–NaOH or LiOH–KOH) hydrothermal method (10), whereas no yield of the layered form was

[1]To whom correspondence should be addressed. E-mail: tabuchi@onri.go.jp.

0022-4596/98 $25.00

detected by ordinary hydrothermal reaction using only Li^+ and Fe^{3+} sources (11) or solvothermal reaction using an α-$NaFeO_2$–$LiOH \cdot H_2O$ mixture (12). The appearance of metastable lithium ferrites could be expected because these hydrothermal/solvothermal reactions can occur below 250°C. In this paper, we examine the structure and magnetic properties of these samples.

2. EXPERIMENTAL

α-$NaFeO_2$ starting material was prepared hydrothermally from a mixture of α-FeOOH (20 g) and an aqueous solution of 50 M NaOH (150 ml) at 220°C and 25–30 kgf/cm^2 for 7 h. To eliminate residual NaOH, the product was washed with ethanol, separated from the solution by filtration, and dried at 100°C. Sample A was prepared from a mixture of α-$NaFeO_2$ (2.0 g) and LiCl (20 g) in ethanol by solvothermal reaction (Table 1). The resulting solids were washed with distilled water, separated by filtration, and dried at 100°C. Sample B was obtained from α-FeOOH (2.7 g) with an excess of $LiOH \cdot H_2O$ (53 g)–KOH (309 g)–distilled H_2O (100 ml) mixed-alkaline aqueous solution by hydrothermal reaction (Table 1). After the reaction, the residual alkaline solutions were removed from the samples using the same procedure as for sample A.

The samples obtained were identified by X-ray diffraction (XRD, Rigaku Rotaflex/RINT), using monochromatized Cu$K\alpha$ radiation. Si powders were used to calibrate 2θ angles ($> 10°$). The diffraction data were collected for 10 s at each 0.02° step over a 2θ range from 10° to 120°. Reflection positions and intensities were calculated for both Cu$K\alpha_1$ and Cu$K\alpha_2$ reflections. A pseudo-Voight profile function was used. Neutron diffraction data were taken on a KPD neutron powder diffractometer at T1-3 at the Tokai Establishment of the Japan Atomic Energy Research Institute. A cylindrical vanadium cell (diameter 10 mm, height 50 mm) was used for the measurements. The wavelength of incident neutrons was fixed at 1.8196 Å by a Ge(331) monochromator. Diffraction data were collected for 30 s at 0.1° step width over a 2θ range from 5° to 155° using 150 ^{3}He proportional counters set at 1° intervals as the neutron detector. The structural parameters for the lithium iron oxides were refined by Rietveld analysis using the computer program RIETAN97-Beta (13).

The Li/Fe, K/Fe, and Na/Fe atomic ratios in the obtained solids were determined by inductively coupled plasma (ICP) emission spectroscopy.

Thermogravimetry–differential thermal analysis (TG–DTA) data were recorded between room temperature and 800°C on both heating and cooling runs. Heating and cooling rates were 10°C/min.

Magnetizations were measured with a magnetic balance (MB-3, Shimadzu) from 83 to 300 K, at magnetic fields between 1.8 and 12.5 kOe using the Faraday method. Since small spontaneous magnetization (M_s) was observed, we subtracted the contribution of M_s to the total magnetization value at each magnetic field between 1.8 and 12.5 kOe in obtaining the magnetic susceptibility data. The temperature and magnetic susceptibility data were calibrated using $(NH_4)_2Mn(SO_4)_3 \cdot 6H_2O$ as the standard. The temperature and field dependence of magnetization were collected down to 5 K by a SQUID magnetometer (Quantum Design, MPMS2). Magnetization curves were also measured between -3 and $+3$ kOe at 300 K using a B–H tracer. γ-Fe_2O_3 powder was used as a standard material for calibrating the magnetization.

^{57}Fe Mössbauer spectra were taken at 300 K (Mössbauer Driving System 1200, Wissel) and below 300 K (CF500, Oxford Instruments). α-Fe foil was used for velocity calibration. Observed spectra were fitted by absorption peaks of Lorentzian line shape.

TABLE 1
Preparation Conditions and Li/Fe, K/Fe, and Na/Fe Ratios for the Samples Prepared by Solvothermal or Hydrothermal Reaction

Sample	Starting mixture	Reaction conditions	Li/Fe ratio	K/Fe or Na/Fe ratio
Sample A	α-$NaFeO_2$–LiCl[a]	220°C, 96 h	0.12	0.03 (Na/Fe)
Sample B	α-FeOOH–LiOH–KOH	220°C, 2 h	0.89	0.01 (K/Fe)

[a]Solvothermal reaction was performed in ethanol instead of distilled water.

3. RESULTS AND DISCUSSION

3.1. Structure and Magnetic Properties of Lithium Iron Oxides Obtained by Solvothermal Reaction

The XRD pattern of sample A (Fig. 1) is similar to that of the inverse spinel ferrites Fe_3O_4 ($Fd\bar{3}m$, $a = 8.396$ Å (14)) and β-$LiFe_5O_8$ ($Fd\bar{3}m$, $a = 8.333$ Å (5)). The values of both the lattice parameter (8.366(10) Å) and the Li/Fe ratio (0.12, Table 1) of sample A are between those of the two spinel ferrites, suggesting the formation of a composition lying in the Fe_3O_4–$LiFe_5O_8$ solid solution ($Li_{1-x}Fe_{5+x}O_8$ ($0 < x < 1$)). The pattern could be fitted by the cubic spinel unit cell $Fd\bar{3}m$ (Fig. 1 and Table 2). Iron occupied 87–94% of both the 8a and 16d sites in the spinel structure, indicating that sample A could be regarded as an inverse spinel such as Fe_3O_4 or $LiFe_5O_8$. This sample has spontaneous magnetization at room temperature like the inverse spinel ferrites mentioned above (Fig. 2). The spontaneous magnetization is formed after solvothermal reaction, because α-$NaFeO_2$ is an antiferromagnet below 11 K (16). The values of spontaneous magnetization and coercive field were estimated to be 39.0(6) G cm^3/g and 130 Oe. The magnetic ordering was also confirmed by Mössbauer spectroscopy at

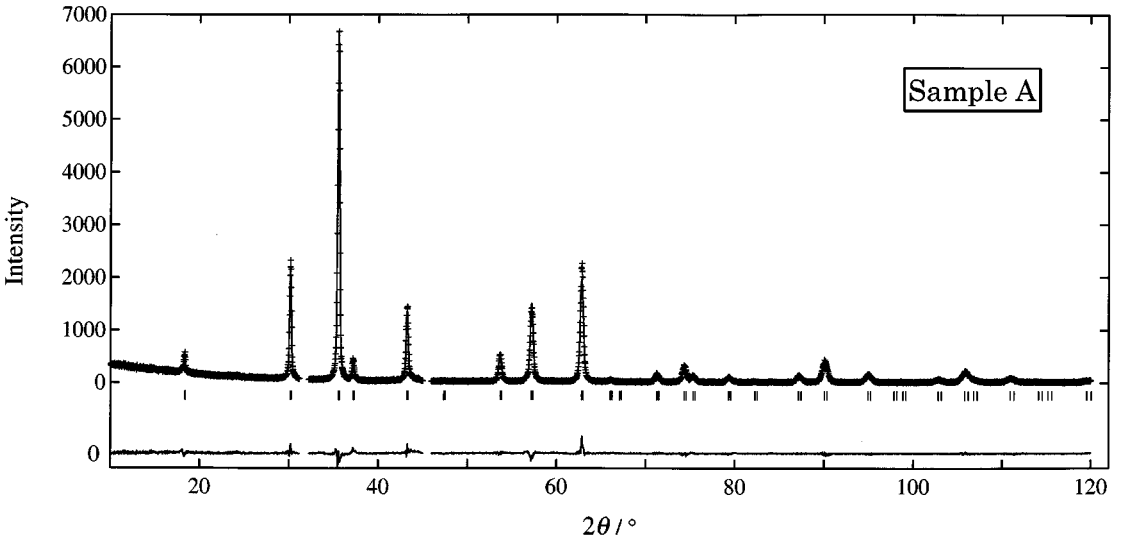

FIG. 1. Observed (+) and calculated (solid line) X-ray diffraction patterns of sample A after solvothermal reaction of α-$NaFeO_2$ and LiCl in ethanol at 220°C for 96 h. The calculated diffraction pattern was constructed from a cubic spinel model ($Fd\bar{3}m$). The difference between the observed and calculated patterns is also shown and given on the same scale. Small peaks of NaCl around 32° and 45° were omitted for the pattern fitting.

300 K (Fig. 3). Overlapping two sextets with different internal fields (H_{int}) is needed to fit the observed spectra. Mössbauer parameters except for the peak area ratio (Table 3) for sample A are similar to those for Fe_3O_4 (17), rather than those for α-$LiFe_5O_8$, which is obtained by heating β-$LiFe_5O_8$ at 700°C (11). Mössbauer parameters for Fe_3O_4 are variable due to the change in Fe^{2+}/Fe^{3+} ratio, which corresponds to the formation of $Fe_{3-x}O_4$ ($0 < x < 0.33$). Volenic *et al.* have proposed that the area ratio of the intensities of the two sextets (M2/M1; see Table 3) depends on the x value in $Fe_{3-x}O_4$ (18). The relation between M2/M1 and x is expressed as follows (18):

$$\mathrm{M2/M1} = (2 - 6x)/(1 + 5x).$$

Using the observed area ratio data for sample A in the above equation, we estimate the x value to be 0.16 ($Fe_{2.84}O_4$). Therefore, the valence state of Fe in sample A is calculated to be 2.82. The valence state value from the Mössbauer spectra is very close to the value (2.87) derived from chemical analysis data (Li/Fe ratio) of sample A ($Li_{0.64}Fe_{5.36}O_8$) assuming that all lithium ions were incorporated into the Fe_3O_4–$LiFe_5O_8$ solid solution. The mixed-valence nature is supported by the fact that sample A is black. This observation indicates that the oxidation state of

TABLE 2
X-Ray Rietveld Refinement Results for Sample A Using the Cubic Spinel Model ($Fd\bar{3}m$)

Atom	Site	g	x	y	z	B (Å^2)
Fe(1)	8*a*	0.94(3)	0	0	0	0.5
Li(1)	8*a*	0.06	0	0	0	$= B$ [Fe(1)]
Fe(2)	16*d*	0.87(3)	0.625	0.625	0.625	$= B$ [Fe(1)]
Li(2)	16*d*	0.13	0.625	0.625	0.625	$= B$ [Fe(1)]
O	32*e*	1	0.8712(11)	0.8712(11)	0.8712(11)	$= B$ [Fe(1)]

Note. g = occupation factor. $a = 8.36209(12)$ Å, $R_{wp} = 11.49\%$, $R_{exp} = 9.12\%$, $R_p = 7.95\%$, $S = 1.26$, $R_I = 4.10\%$, $R_F = 2.36\%$, scale factor = $1.92(2) \times 10^{-5}$.

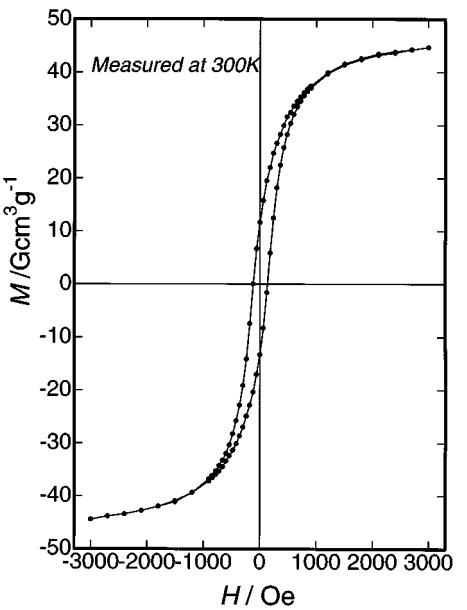

FIG. 2. Field dependence of the magnetization at 300 K for sample A.

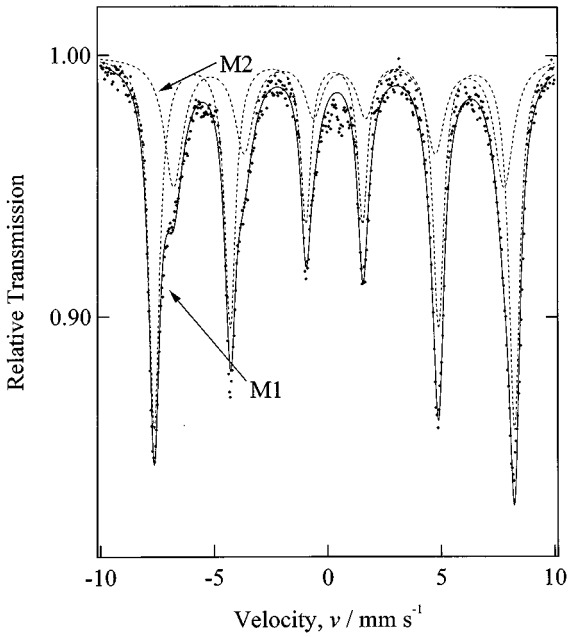

FIG. 3. Observed (●) and calculated (solid line) ^{57}Fe Mössbauer spectra at 300 K for sample A. The component sextets, named M1 and M2, for constructing the calculated spectrum are shown as broken line.

iron in our sample can be reduced from +3 during prolonged solvothermal reaction. A similar spinel phase was observed previously by Uchida *et al.* (19), who obtained $Li_{0.36}Fe_{5.64}O_8$ ($Fd\bar{3}m$, $a = 8.373$ Å) from α-Fe in 2 M LiOH solution by hydrothermal reaction at 250°C for 50 h. The formation of the spinel ferrites from α-$NaFeO_2$ by ion-exchange reaction in molten salt has been reported by Blesa *et al.* (20, 21). Although they observed the presence of iron on tetrahedral 8*a* sites in their nickel and magnesium ferrites, they made no comment regarding the presence of ferrous ion in the spinel structure.

The thermal stability of both samples was checked by TG–DTA measurement up to 800°C in air (Fig. 4). A weight gain was detected from 100 to 300°C on heating, which

TABLE 3
Mössbauer Parameters for Sample A Compared with the Data for Fe_3O_4 and α-$LiFe_5O_8$ with Inverse Spinel Structure at 300 K

Sample	Component	IS (mm s^{-1})	QS (mm s^{-1})	Γ (mm s^{-1})	H_{int} (T)	Area ratio (%)
Sample A	M1	+0.33	−0.011	0.58	49	63
	M2	+0.55	−0.042	1.00	45	37
Fe_3O_4	M1	+0.26	−0.02	—	49	33
	M2	+0.67	0.00	—	46	67
α-$LiFe_5O_8$	M1	+0.39	+0.02	0.38	51	60
	M2	+0.18	−0.05	0.35	50	40

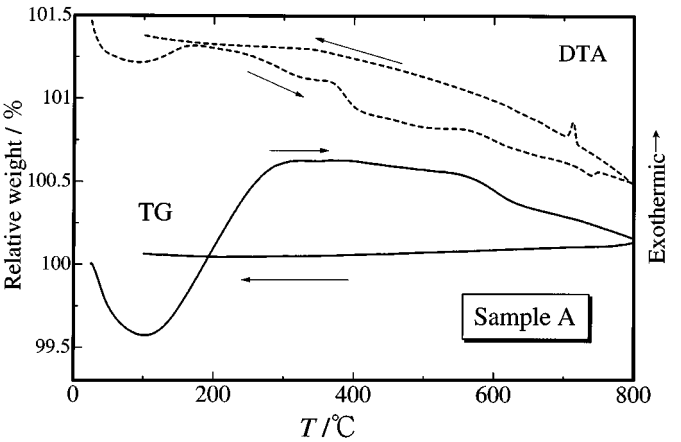

FIG. 4. TG–DTA curves for sample A between 20 and 800°C in air.

corresponds to the oxidation of the sample, because a mixture of α-Fe_2O_3 and $LiFe_5O_8$ was obtained after heating at 400°C for 5 h. Complete oxidation of sample A to Fe^{3+} materials would lead to a weight gain of 1.33% from $Li_{0.64}Fe_{5.36}O_8$ to $Li_{0.64}Fe_{5.36}O_{8.36}$, which is close to the value (1.04%) obtained from TG experiments on heating to 300°C. The appearance of endothermic/exothermic peaks around 700°C on heating/cooling runs can be attributed to the α–β transition of $LiFe_5O_8$ (15). The formation of lithium iron oxides with inverse spinel structure implies that ideal ion-exchange reaction is difficult to accomplish due to moving Fe^{3+} ions to tetrahedral sites in a ccp oxygen array.

3.2. Structure and Magnetic Properties of Lithium Iron Oxides Obtained by Mixed-Alkaline Hydrothermal Reaction

The neutron diffraction patterns (Fig. 5) for sample B were well fitted by a two-phase mixture of 84% layered $LiFeO_2$ (α-$NaFeO_2$ type structure, $R\bar{3}m$) and 16% α-$LiFeO_2$ ($Fm3m$) (Table 4), indicating that sample B contains mainly layered $LiFeO_2$. The observed lattice parameters are close to previous data for layered $LiFeO_2$ ($a = 2.9632(7)$ Å, $c = 14.636(4)$ Å (9)) and α-$LiFeO_2$ ($a = 4.158$ Å (1)).

SEM (Fig. 6) shows that sample B consists of crystal like particles, indicating that they were precipitated from the aqueous solution. The magnetic field dependence of magnetization at 83 and 300 K (Fig. 7a) showed that the spontaneous magnetization values were less than 0.1 G cm^3/g, which means that there is only a negligible contribution of ferro- or ferrimagnetic impurities (β-$LiFe_5O_8$, α-Fe_2O_3, γ-Fe_2O_3, Fe_3O_4) to the magnetic data above 83 K. The linear temperature dependence of the inverse molar susceptibility (Fig. 7b) indicates a Curie–Weiss paramagnetic behavior. Applying the Curie–Weiss law to χ_m^{-1} vs T data above 83 K, we estimate the μ_{eff} and θ values to be 5.680(6) μ_B and

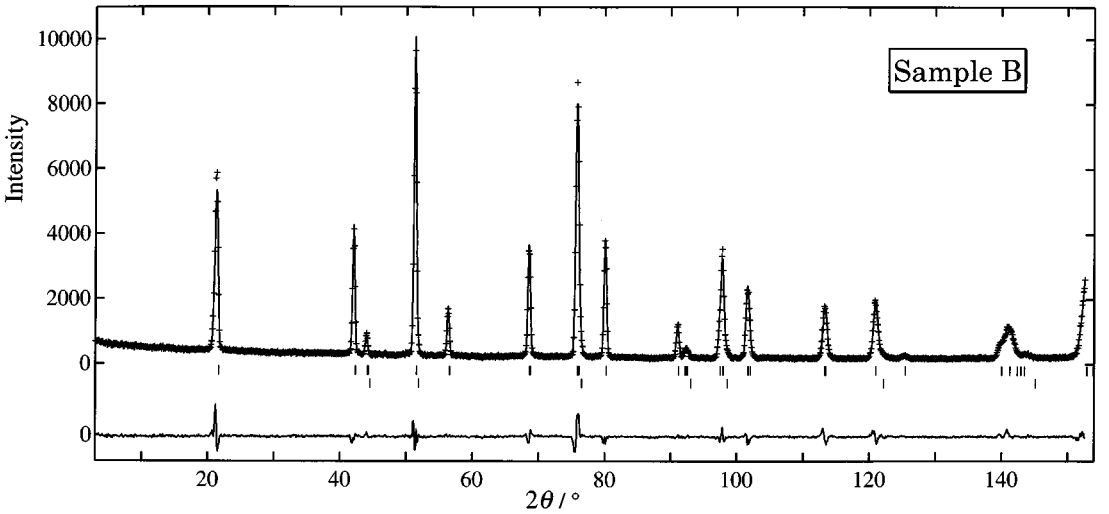

FIG. 5. Observed (+) and calculated (solid line) neutron diffraction patterns for sample B. The calculated pattern was constructed from a two-phase model consisting of layered rock salt ($R\bar{3}m$) and cubic rock salt ($Fm3m$) unit cells. The difference between the two patterns is also shown and given on the same scale. Peak positions of layered $LiFeO_2$ (upper vertical marks) and α-$LiFeO_2$ (lower vertical marks) are indicated just below the patterns.

+ 19 K, respectively. The μ_{eff} value is close to the spin-only value (5.92 μ_B) of high-spin Fe^{3+} and that of α-$NaFeO_2$ (5.8 μ_B (16)). The sample positive θ value suggests the presence of ferromagnetic interaction between Fe^{3+} ions.

The temperature dependence of the normalized magnetization between 5 and 200 K (Fig. 8) reveals a cusp at 20 K at both low and high applied fields on zero-field-cooling (ZFC) and field-cooling (FC) runs without hysteresis. The large difference in magnetic behavior between sample B and the other form of $LiFeO_2$ was detected because α-, β- and γ-$LiFeO_2$ are antiferromagnets below 90–280 K (12, 22). M/H vs T data of sample B are similar to those of α-$NaFeO_2$, which is an antiferromagnet below 11 K (16). The higher Néel point of layered $LiFeO_2$ than that of α-$NaFeO_2$ may be caused by the difference in the interlayer distance of FeO_6 slabs in the layered rock salt structure, because the c parameter for layered $LiFeO_2$ (14.5212(9) Å) is much smaller than 16.100(2) Å for α-$NaFeO_2$, compared with the difference in the a parameter (2.95362(14) Å for $LiFeO_2$, 3.0264(3) Å for $NaFeO_2$). No spin-glass-like behavior was detected for layered $LiFeO_2$, contrary to $LiNiO_2$ (23).

TABLE 4

Neutron Rietveld Refinement Results for Sample B Using a Two-Phase Model of (a) Layered $LiFeO_2$ ($R\bar{3}m$) and (b) α-$LeFeO_2$ ($Fm3m$)

Atom	Site	g	x	y	z	B (Å^2)
			(a) Layered $LiFeO_2$[a]			
Li	3*a*	1	0	0	0	1.7(9)
Fe	3*b*	1	0	0	0.5	0.5(2)
O	6*c*	1	0	0	0.2424(9)	0.4(2)
			(b) α-$LiFeO_2$[b]			
Li/Fe	4*a*	1	0	0	0	0.5
O	4*b*	1	0.5	0.5	0.5	0.5

Note. Mass fraction of compounds, layered $LiFeO_2$:α-$LiFeO_2$ = 0.84:0.16.

[a] g = occupation factor. a = 2.95362(14) Å, c = 14.5212(9) Å, R_{wp} = 8.85%, R_{exp} = 4.64%, R_p = 6.89%, S = 1.91, R_I = 2.44%, R_F = 1.35%, scale factor = $3.82(4) \times 10^{-2}$.

[b] g = occupation factor. a = 4.1620(3) Å, R_{wp} = 8.85%, R_{exp} = 4.64%, R_p = 6.89%, S = 1.91, R_I = 2.12%, R_F = 1.04%, scale factor = $2.98(10) \times 10^{-2}$. Occupation factor of both Li and Fe were fixed to be 0.5 during refinement.

The Mössbauer spectra for sample B (Fig. 9) seemed to change from a doublet to a sextet below 20 K with decreasing temperature, confirming that the cusp at 20 K (Fig. 8) is the Néel point (T_N) for layered $LiFeO_2$. A small and broad sextet was observed with a doublet in the 30 K spectrum, and the sextet could be fitted by superimposing two sextets with different internal fields (H_{int} = 46 and 41 T, Table 5) and quadrupole splitting. This means that the presence of another phase with T_N between 30 and 150 K (phase 2 in Table 5) must be included. The observed 5 K spectrum could be fitted by three sextets consisting of two sextets for phase 2 (14% of total fraction) and a sextet for phase 1 (layered $LiFeO_2$, 86% of total fraction), because two sextets with different internal fields (51 and 48 T) are needed to fit the spectrum of α-$LiFeO_2$ (T_N = 90 K) at 5 K (12). Superimposing spectra of 83–90% of layered $LiFeO_2$ and 10–17% of α-$LiFeO_2$ could fit all Mössbauer spectra below 300 K. If phase 2 is only α-$LiFeO_2$, the fraction of these two phases is very close to the neutron Rietveld analysis results. The internal fields at 5 K and the isomer shift values at 300 K

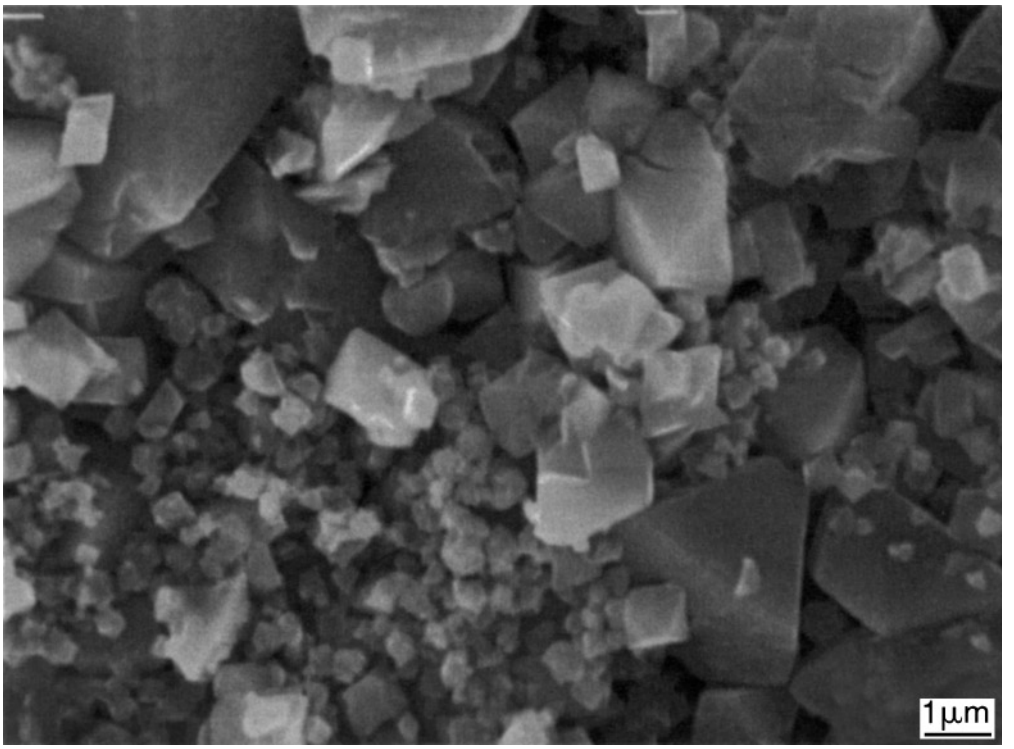

FIG. 6. Scanning electron microscope photograph of sample B.

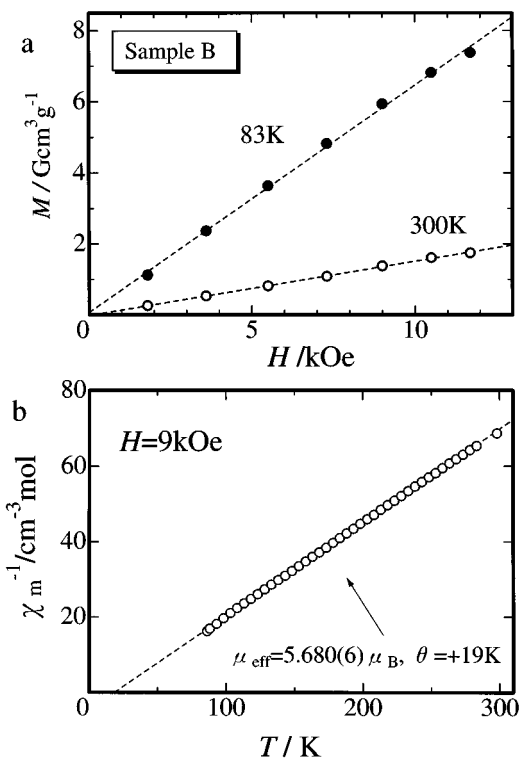

FIG. 7. Field dependence of magnetization at 83 and 300 K (a) and temperature dependence of inverse molar susceptibility between 86 and 300 K (b) for sample B.

revealed that sample B consisted of high-spin Fe^{3+} compounds, indicating that iron valency is kept during the mixed-alkaline hydrothermal reaction, contrary to the case of the solvothermal reaction.

4. CONCLUSION

Preparation routes to lithium iron oxides using hydrothermal/solvothermal reaction at 220–230°C are sum-

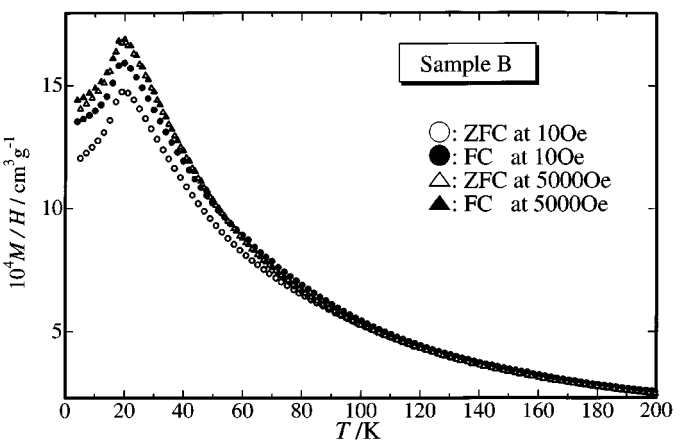

FIG. 8. Temperature dependence of magnetization normalized by magnetic field on zero-field cooling (ZFC) and field-cooling (FC) runs at two different magnetic fields for sample B (5–200 K).

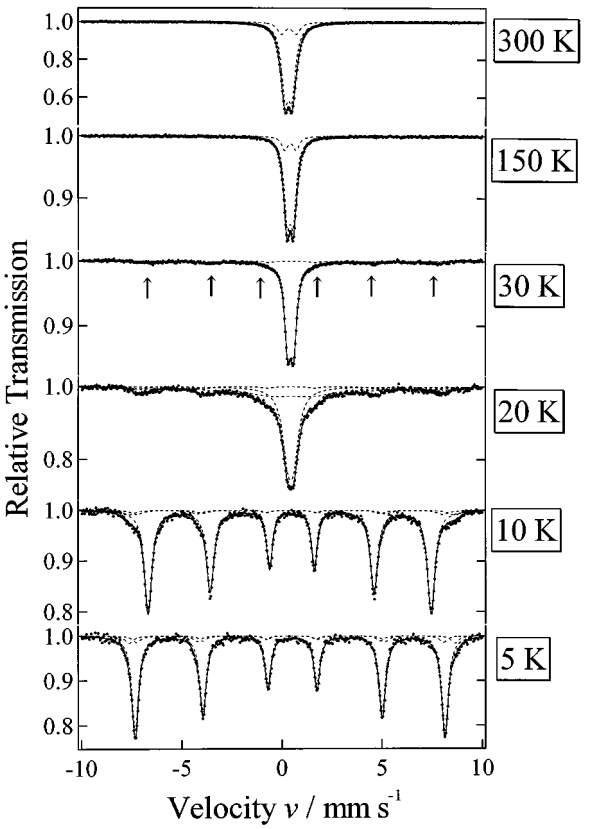

FIG. 9. Observed (●) and calculated (solid line) ^{57}Fe Mössbauer spectra at 300, 150, 30, 20, 10, and 5 K for sample B. Each doublet or sextet for fitting the observed spectra is expressed as a broken line. The Mössbauer parameters are listed in Table 5. The arrows show the presence of a broad sextet at 30 K.

TABLE 5
Mössbauer Parameters for Sample B below 300 K

T (K)	IS (mm s^{-1})	QS (mm s^{-1})	Γ (mm s^{-1})	H_{int} (T)	Area ratio (%)
300	+0.35	0.34	0.44	—	83 (phase 1)
	+0.36	0.74	0.47	—	17 (phase 2)
150	+0.44	0.30	0.37	—	85 (phase 1)
	+0.45	0.58	0.35	—	15 (phase 2)
30	+0.47	0.30	0.37	—	84 (phase 1)
	+0.42	+0.026	0.66	46	8 (phase 2)
	+0.42	−0.077	0.66	41	7 (phase 2)
20	+0.47	0.30	0.63	—	51 (phase 1)
	+0.44	−0.13	1.13	43	37 (phase 1)
	+0.44	+0.026	0.66	48	6 (phase 2)
	+0.43	−0.077	0.66	46	6 (phase 2)
10	+0.47	−0.13	0.45	44	89 (phase 1)
	+0.50	+0.026	0.68	50	6 (phase 2)
	+0.46	−0.078	0.68	47	5 (phase 2)
5	+0.49	−0.13	0.40	48	86 (phase 1)
	+0.51	+0.026	0.44	51	7 (phase 2)
	+0.48	−0.078	0.44	48	7 (phase 2)

Note. Phase 1 has a magnetic transition temperature of 20 K, whereas phase 2 has a magnetic transition temperature between 30 and 150 K.

marized in Fig. 10. Well-known lithium iron oxides, the α, β, and γ polymorphs of $LiFeO_2$ and β-$LiFe_5O_8$, were obtained by hydrothermal reaction between Fe^{3+} sources and lithium hydroxide below 250°C. The transformation from the α to the γ polymorph could occur during prolonged hydrothermal reaction of $FeCl_3 \cdot 6H_2O$ and $LiOH \cdot H_2O$ (24). The metastable $Li_{1-x}Fe_{5+x}O_8$ phase with spinel-related structure could be isolated by the solvothermal ion-exchange reaction of α-$NaFeO_2$ with anhydrous LiCl in ethanol. The metastable layered $LiFeO_2$ with a small amount of α-$LiFeO_2$ was obtained from α-FeOOH by a one-step process using a mixed-alkaline hydrothermal reaction. Optimization of starting materials, including solvent and its combination ratios, is very important to obtain

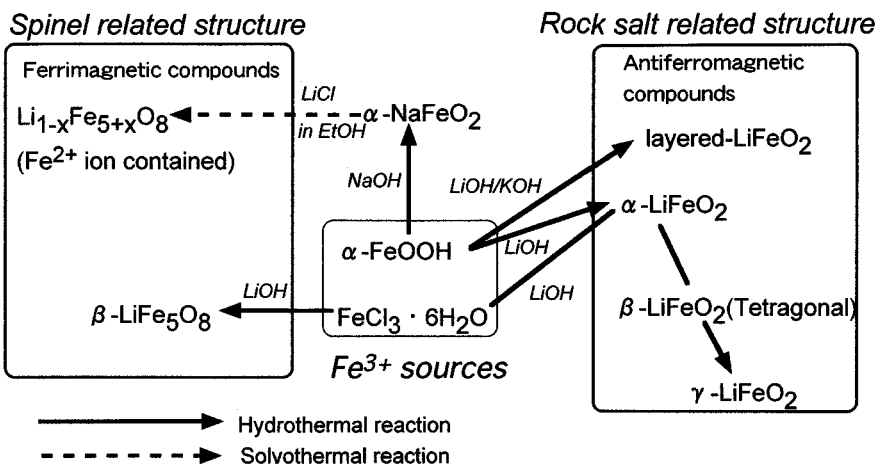

FIG. 10. Preparation routes to the lithium iron oxides using solvothermal and hydrothermal reactions.

many polymorphs of lithium iron oxides, including metastable phases.

The solvothermally obtained spinel phases have spontaneous magnetization at 300 K due to the presence of iron in the 8*a* site and decomposed readily by heating at 400°C in air. The layered polymorph, like α-$NaFeO_2$, exhibited antiferromagnetic behavior below 20 K but no spin-glass-like behavior, as reported for $LiNiO_2$. Its Néel temperature (T_N) is lower than those of other $LiFeO_2$ polymorphs (α, β, and γ) with NaCl-related structure ($90 < T_N < 300$ K), suggesting that antiferromagnetic ordering could be suppressed by the formation of an α-$NaFeO_2$ type structure.

REFERENCES

1. J. C. Anderson and M. Schieber, *J. Phys. Chem. Solids* **25,** 961 (1964).
2. M Brunel and F. de Bergevin, *J. Phys. Chem. Solids* **29,** 163 (1968).
3. R. Famery, P. Bassoul, and F. Queyroux, *J. Solid State Chem.* **57,** 178 (1985).
4. R. Kanno, T. Shirane, Y. Kawamoto, Y. Takeda, M. Takano, M. Ohashi, and Y. Yamaguchi, *J. Electrochem. Soc.* **143,** 2435 (1996).
5. Y. Sakurai, H. Arai, S. Okada, and J. Yamaki, *J. Power Sources* **68,** 711 (1997).
6. V. Nalbandian and I. Sukaev, *Russ. J. Inorg. Chem.* (*Eng. Transl.*) **32,** 453 (1987).
7. S. Kikkawa, H. Okura, and M. Koizumi, *Mater. Chem. Phys.* **18,** 375 (1987).
8. B. Fuchs and S. Kemmer-Sack, *Solid State Ionics* **68,** 279 (1994).
9. T. Shirane, R. Kanno, Y. Kawamoto, Y. Takeda, M. Takano, T. Kamiyama, and F. Izumi, *Solid State Ionics* **79,** 227 (1995).
10. K. Ado, M. Tabuchi, H. Kobayashi, O. Nakamura, Y. Inaba, R. Kanno, M. Takagi, and Y. Takeda, *J. Electrochem. Soc.* **144,** L177 (1997).
11. M. Tabuchi, K. Ado, H. Sakaebe, C. Masquelier, H. Kageyama, and O. Nakamura, *Solid State Ionics* **79,** 220 (1995).
12. M. Tabuchi, C. Masquelier, T. Takeuchi, K. Ado, I. Matsubara, T. Shirane, R. Kanno, S. Tsutsui, S. Nasu, H. Sakaebe, and O. Nakamura, *Solid State Ionics* **90,** 129 (1996).
13. F. Izumi, *in* "The Rietveld Method" (R. A. Young, Ed.), Chap. 13. Oxford Univ. Press, Oxford, 1993.
14. JCPDS Powder Diffraction File 19-6729.
15. M. Schieber, *J. Inorg. Nucl. Chem.*, **26,** 1363 (1964).
16. T. Ichida, T. Shinjo, Y. Bando, and T. Takada, *J. Phys. Soc. Jpn.* **29,** 795 (1970).
17. E. Murad and J. H. Johnston, *in* "Mössbauer Spectroscopy Applied to Inorganic Chemistry," (G. J. Long, Ed.), Vol. 2, pp. 507–582. Plenum, New York, 1984.
18. K. Volenic, M. Seberini, and J. Neid, *Czech. J. Phys. B* **25,** 1063 (1975).
19. S. Uchida, H. Hashiwagi, T. Sato, and A. Okuwaki, *J. Mater. Sci.* **31,** 3827 (1996).
20. M. C. Blesa, E. Morán, U. Amador, and N. H. Anderson, *J. Solid State Chem.* **129,** 123 (1997).
21. M. C. Blesa, U. Amador, E. Morán, N. Menéndez, J. D. Tornero, and J. Rodríguez-Carvajal, *Solid State Ionics* **63–65,** 429 (1993).
22. D. E. Cox, G. Shirane, P. A. Flinn, S. L. Ruby, and W. J. Takei, *Phys. Rev.* **132,** 1547 (1963).
23. K. Yamaura, M. Takano, A. Hirano, and R. Kanno, *J. Solid State Chem.* **127,** 109 (1996).
24. C. Barriga, V. Barron, R. Gancedo, M. Gracia, J. Morales, J. L. Tirado, and J. Torrent, *J. Solid State Chem.* **77,** 132 (1988).